

## STUDIES OF DARK RESONANCES IN Rb ATOMS IN THE FIELD OF LIGHT PULSE TRAIN

M. AUZINSH,<sup>1</sup> R.A. MALITSKIY,<sup>2</sup> I.V. MATSNEV,<sup>2</sup> A.M. NEGRIYKO,<sup>2</sup>  
V.I. ROMANENKO,<sup>2</sup> V.M. KHODAKOVSKYY,<sup>2</sup> L.P. YATSENKO<sup>2</sup>

<sup>1</sup>Department of Physics, University of Latvia  
(19, Rainis Blvd., Riga LV-1586, Latvia)

<sup>2</sup>Institute of Physics, Nat. Acad. of Sci. of Ukraine  
(46, Nauky Ave., Kyiv 03680, Ukraine; e-mail: vr@iop.kiev.ua)

PACS 42.50.Gy; 32.80.Bx  
©2009

Dark resonances in  $^{87}\text{Rb}$  vapor in the field of a femtosecond laser pulse train have been studied theoretically and experimentally. Three- and four-level schemes of interaction between an  $^{87}\text{Rb}$  atom and the field, which are formed by the field-coupled magnetic sublevels of states  $^2S_{1/2}$  and  $^3P_{3/2}$  of the rubidium atom have been analyzed. The position and the shape of the experimentally recorded dark resonance correspond to the results of our calculations. It has been shown that the interaction between rubidium vapor and a polychromatic field allows the signal to be enhanced substantially in comparison with that in the case of bichromatic field.

### 1. Introduction

The study of phenomena resulting from the coherence of atomic and molecular quantum states attracted the attention of researchers for last three decades. One of the most interesting among them is the coherent trapping of population [1–3]. Population trapping reveals itself experimentally as a reduction of the atomic fluorescence intensity under the influence of two fields, which couple two long-lived atomic states (one of which can be the ground state) with a short-lived excited state in a narrow frequency interval, when the frequency of either field changes. This dip in the fluorescence intensity plot is observed, if the difference between the frequencies of light fields acting upon the atom is so that the energy difference between their quanta is equal to the difference between the energies of long-lived state levels (the condition of two-photon resonance). This phenomenon is referred to as a “dark resonance” [4]. The physical basis of the population trapping is a possibility for a “dark state”, which emerges owing to a superposition of long-lived states, to be formed in the system “atom + field”; the atom in such a state does not emit. The dark resonance width is governed by the duration of the atom–field interaction and the relaxation times of the density matrix elements which describe the long-lived state. It can be very narrow (in a rubidium cell filled with a buffer

gas, there were observed resonances 30 Hz in width [5]). Such resonances are of great interest in the domains of frequency standards [6] and magnetometry [7, 8].

For today, still poorly studied remains the interaction between an atom and a polychromatic field, the Fourier components of which can form a dark resonance. In this respect, fields with equidistant spectral components, i.e. the sequences of light pulses with a fixed repetition frequency, are most interesting. By so selecting the repetition frequency that the difference between the energies of two lower levels is multiple of it, a dark resonance can be observed [9, 10].

In 1999, there appeared a possibility to effectively generate a “frequency comb” which overlaps a wide frequency range by equidistant frequency components. Such a spectrum is generated, for instance, by femtosecond lasers. The fixed time interval between laser pulses determines the frequency shift between the “comb” components, and the wide spectral range is provided by a small duration of laser pulses. The frequency comb is widely used today in metrology, mainly for optical frequency measurements [11]. Besides its application in metrology, the “frequency comb” can be used in experiments, where the coherent interaction between laser light and atoms is studied. Let the width of the frequency comb exceed the frequency  $\omega_{12}$  that corresponds to the difference between the energies of long-lived states. If the difference between the “comb” frequency components  $\Omega_m$  is so selected that  $N\Omega_m \approx \omega_{12}$ , where  $N$  is an integer, then, provided  $N\Omega_m = \omega_{12}$ , the coherent trapping of population and, respectively, a dip in the fluorescence spectrum can be expected, if the interval between frequency components is varied in the vicinity of  $\Omega_m = \omega_{12}/N$  [9].

The most complete – to date – research of dark resonances in the field of a light pulse train was carried out in work [9], using Rb atoms as an example. With the help of a numerical simulation of the interaction between an atom and the field of a sequence of light pulses with the

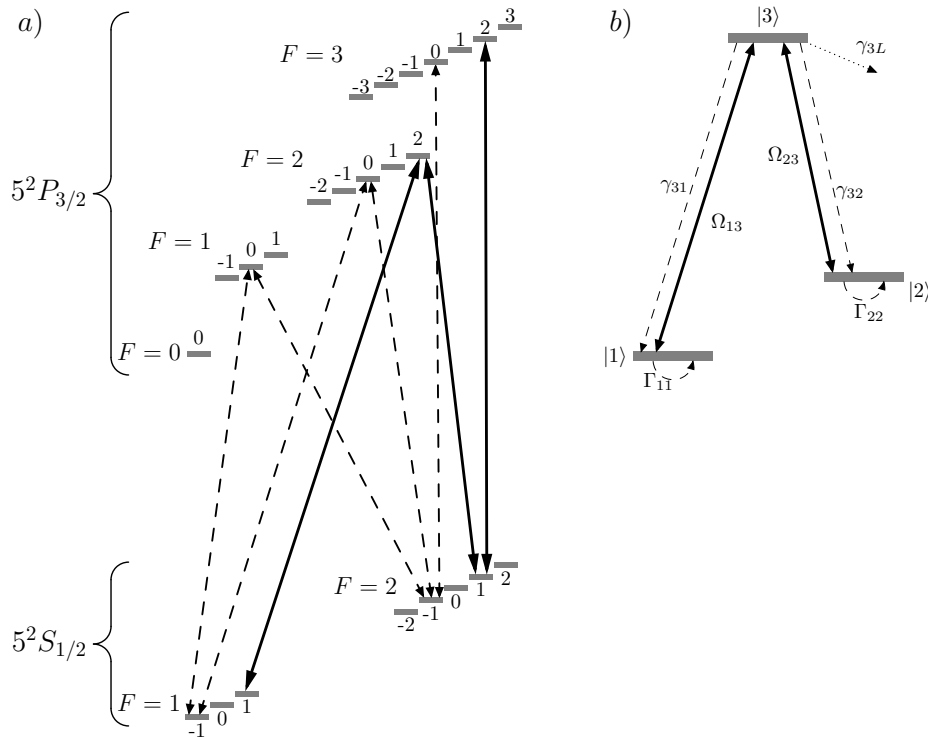


Fig. 1. (a) Energy level diagram for  $^{87}\text{Rb}$  atom. Each level of the superfine structure with the total momentum  $F$  is degenerate with multiplicity  $2F + 1$ . Dashed arrows correspond to allowed transitions under the action of  $\sigma^+$ -polarized radiation from states  $|^2S_{1/2}, F = 1, m = -1\rangle$  and  $|^2S_{1/2}, F = 2, m = -1\rangle$ , and solid arrows correspond to allowed transitions from states  $|^2S_{1/2}, F = 1, m = 1\rangle$  and  $|^2S_{1/2}, F = 2, m = 1\rangle$ . In the latter case, the interaction between the atom and the field can be described by the  $\Lambda$ -scheme (b), because estimations show that the transition  $|^2S_{1/2}, F = 2, m = 1\rangle \rightarrow |^2P_{3/2}, F = 3, m = 2\rangle$  is far from the resonance with the Fourier components of the field. In panel b, symbols  $|1\rangle$ ,  $|2\rangle$ , and  $|3\rangle$  denote states  $|^2S_{1/2}, F = 1, m = 1\rangle$ ,  $|^2S_{1/2}, F = 1, m = 1\rangle$ , and  $|^2P_{3/2}, F = 2, m = 2\rangle$ , respectively. Constants  $\gamma_{31}$  and  $\gamma_{32}$  are the rates of spontaneous transitions into states  $|1\rangle$  and  $|2\rangle$ , respectively; the Rabi frequencies  $\Omega_{13}$  and  $\Omega_{23}$  describe the interaction between the atom and the field

carrier frequency close to the frequency of  $D1$ -transition in rubidium, it was shown that dark resonances can be observed, if the energy difference between the superfine structure components is multiple of the pulse repetition frequency  $\nu$ . At the same time, the authors of work [9] left real conditions of the experiment beyond the scope of their consideration, namely, the fact that the field interacts with an ensemble of atoms with various velocities. The distribution of atoms over velocities was taken into account in work [5], where the interaction between a rubidium atom and a bichromatic field with the frequencies close to the frequency of  $D2$ -transition in rubidium was studied. However, the assumptions made in this work to make the analysis simpler – namely, identical values of Rabi frequencies, which describe the atom–field interaction, and identical probabilities of spontaneous transitions from superfine structure levels of the excited state onto those of the ground state – were not adequate to real experimental conditions. Therefore, the study of the

interaction between a rubidium atom and a light pulse train, which would use real spectroscopic constants that describe the atom–field interaction and consider the distribution of atoms over their velocities, is challenging.

## 2. Model of Atom–Field Interaction

The scheme of Rb atom energy levels, which are responsible for  $D2$ -line in the rubidium spectrum ( $\lambda = 780$  nm), is shown in Fig. 1 [13]. Every level of the superfine structure with the total momentum  $F$  is split into  $2F + 1$  sublevels which are described by the quantum number  $m$  ( $m = -F, -F + 1, \dots, F - 1, F$ ) and, if the atom is subjected to a magnetic field, have different energies. We assume that the atom is subjected to the circularly polarized ( $\sigma^+$ -polarization) radiation of a laser which generates a sequence of light pulses with period  $T$ . If the frequency difference between magnetic sublevels with an identical  $m$ -value of states  $|^2S_{1/2}, F = 1\rangle$

and  $|^2S_{1/2}, F = 2\rangle$  coincides with  $N$  times the repetition frequency of light pulses, the dark resonance – a reduction of the rubidium atom fluorescence intensity – can be observed.

As is seen from Fig. 1, *a*, states  $|^2S_{1/2}, F = 1\rangle$  and  $|^2S_{1/2}, F = 2\rangle$  with the magnetic quantum number  $m = -1$  are coupled by the  $\sigma^+$ -polarized laser radiation with states  $|^2P_{3/2}, F = 1\rangle$ ,  $|^2P_{3/2}, F = 2\rangle$ , and  $|^2P_{3/2}, F = 3\rangle$  with  $m = 0$ . The coupling between those states depends on a detuning of the closest, by frequency, Fourier component of the field from a resonance with the frequency of the corresponding transition. In addition, the excitation of state  $|^2P_{3/2}, F = 2\rangle$  with  $m = 0$  is possible. At the same time, states  $|^2S_{1/2}, F = 1\rangle$  and  $|^2S_{1/2}, F = 2\rangle$  with the magnetic quantum number  $m = 1$  are coupled by the  $\sigma^+$ -polarized laser radiation with states  $|^2P_{3/2}, F = 2\rangle$  and  $|^2P_{3/2}, F = 3\rangle$  with  $m = 2$ . Under the experimental conditions, the latter state is excited insignificantly, so that, for transitions from sublevels with  $m = 1$ , the interaction between the atom with the field can be analyzed in the framework of the three-level atomic model (Fig. 1, *b*).

The probability of that or another transition is determined by the electric field strength of laser radiation, the matrix elements of the corresponding transition, and the frequency difference between this transition and the closest Fourier component in the spectrum of laser radiation. If the magnetic field does not act upon the atom, all probable transitions form dark resonances on the dependence of the atomic fluorescence intensity on the pulse repetition frequency  $\nu = 1/T$  at identical frequency values. Provided that the transitions are weakly saturated, the populations at magnetic sublevels of the ground state are slightly different from their equilibrium values, and the result of the interaction between atoms and the field can be found in most cases, by considering the three-level schemes of atom–field interaction independently and then summing up the populations found for the magnetic sublevels of the excited state. An exception is the interaction of atoms with the field of such a pulse train, when the transitions between states  $|^2S_{1/2}, F = 1, m\rangle$ ,  $|^2S_{1/2}, F = 2, m\rangle$ , and  $|^2P_{3/2}, F = 1, m'\rangle$ , as well as between states  $|^2S_{1/2}, F = 1, m\rangle$ ,  $|^2S_{1/2}, F = 2, m\rangle$ , and  $|^2P_{3/2}, F = 2, m'\rangle$ , where  $m' = m, m \pm 1$ , are simultaneously close to the resonance (with different Fourier components of the field). In this case, the analysis of two different  $\Lambda$ -schemes of the atom–field interaction is needed, in which two magnetic sublevels coincide in the ground state and differ from each other in the excited one.

Now, let us analyze how a rubidium atom interacts with the  $\sigma^+$ -polarized field. Consider the transitions which are most favorable for the formation of dark resonances:  $|^2S_{1/2}, F = 1, m = 1\rangle \rightarrow |^2P_{3/2}, F = 2, m = 2\rangle$  and  $|^2S_{1/2}, F = 2, m = 1\rangle \rightarrow |^2P_{3/2}, F = 2, m = 2\rangle$  (see Fig. 1). To make the form of the equations for the density matrix – they are given below – simpler, we introduce the notations  $|1\rangle = |^2S_{1/2}, F = 1, m = 1\rangle$ ,  $|2\rangle = |^2S_{1/2}, F = 1, m = 1\rangle$ , and  $|3\rangle = |^2P_{3/2}, F = 2, m = 2\rangle$ . We neglect the transition  $|^2S_{1/2}, F = 2, m = 1\rangle \rightarrow |^2P_{3/2}, F = 3, m = 2\rangle$ , because the Fourier component of the field, which is closest to its frequency, is far from resonance. Hence, the equations for density matrix evolution look like

$$\frac{d}{dt}\rho_{11} = \frac{i\mathcal{E}}{\hbar} (d_{13}\rho_{31} - d_{31}\rho_{13}) - \Gamma_{11} (\rho_{11} - \rho_{11}^{(0)}) + \gamma_{31}\rho_{33},$$

$$\frac{d}{dt}\rho_{22} = \frac{i\mathcal{E}}{\hbar} (d_{23}\rho_{32} - d_{32}\rho_{23}) - \Gamma_{22} (\rho_{22} - \rho_{22}^{(0)}) + \gamma_{32}\rho_{33},$$

$$\frac{d}{dt}\rho_{33} = \frac{i\mathcal{E}}{\hbar} (d_{31}\rho_{13} - d_{13}\rho_{31} + d_{32}\rho_{23} - d_{23}\rho_{32}) -$$

$$- (\gamma_{31} + \gamma_{32} + \gamma_{3L}) \rho_{33},$$

$$\frac{d}{dt}\rho_{12} = \frac{i\mathcal{E}}{\hbar} (d_{13}\rho_{32} - d_{32}\rho_{13}) + \frac{i}{\hbar} (W_2 - W_1) \rho_{12} -$$

$$- \frac{1}{2} (\Gamma_{11} + \Gamma_{22}) \rho_{12},$$

$$\frac{d}{dt}\rho_{13} = \frac{i\mathcal{E}}{\hbar} (d_{13} [\rho_{33} - \rho_{11}] - d_{23}\rho_{12}) + \frac{i}{\hbar} (W_3 -$$

$$- W_1) \rho_{13} - \frac{1}{2} (\gamma_{31} + \gamma_{32} + \gamma_{3L} + \Gamma_{11}) \rho_{13},$$

$$\frac{d}{dt}\rho_{23} = \frac{i\mathcal{E}}{\hbar} (d_{23} [\rho_{33} - \rho_{22}] - d_{13}\rho_{21}) + \frac{i}{\hbar} (W_3 -$$

$$W_2) \rho_{23} - \frac{1}{2} (\gamma_{31} + \gamma_{32} + \gamma_{3L} + \Gamma_{22}) \rho_{23},$$

$$\rho_{21} = \rho_{12}^*, \quad \rho_{31} = \rho_{13}^*, \quad \rho_{32} = \rho_{23}^*, \quad (1)$$

where  $d_{13}$ ,  $d_{31}$ ,  $d_{23}$ , and  $d_{32}$  are the matrix elements of dipole moment; and  $W_1$ ,  $W_2$ , and  $W_3$  are the energies

of states  $|1\rangle$ ,  $|2\rangle$ , and  $|3\rangle$ , respectively. Let the concentration of rubidium vapor be so low that the collision-induced relaxation can be neglected. As a result, the relaxation rate for the density matrix elements is determined by the rate of spontaneous radiation emission from state  $|3\rangle$  with transitions into states  $|1\rangle$ ,  $|2\rangle$ , and others, differing from those two ( $\gamma_{31}$ ,  $\gamma_{32}$ , and  $\gamma_{3L}$ , respectively), as well as by the time  $\tau_{\text{tr}}$  needed for a flying atom to cross the laser beam ( $\Gamma_{11} = \Gamma_{22} = \tau_{\text{tr}}^{-1}$ ). Proceeding from the condition that, in the absence of laser radiation, all magnetic sublevels of state  $^2S_{1/2}$  are populated identically, we obtain

$$\rho_{11}^{(0)} = \rho_{22}^{(0)} = \frac{1}{8}. \quad (2)$$

Let the inverse lifetime in state  $|3\rangle$  be equal to  $\gamma$ . Then,  $\gamma_{3L}$  is determined from the equation

$$\gamma_{31} + \gamma_{32} + \gamma_{3L} = \gamma, \quad (3)$$

and  $\gamma_{31}$  and  $\gamma_{32}$  from the equations

$$\gamma_{31} = \gamma \frac{|\langle ^2P_{3/2}, F=2, m=2 | \mathbf{d} | ^2S_{1/2}, F=1, m=1 \rangle|^2}{\sum_{F'=1}^2 \sum_{m'=-F'}^{F'} |\langle ^2P_{3/2}, F=2, m=2 | \mathbf{d} | ^2S_{1/2}, F', m' \rangle|^2},$$

$$\gamma_{32} = \gamma \frac{|\langle ^2P_{3/2}, F=2, m=2 | \mathbf{d} | ^2S_{1/2}, F=2, m=1 \rangle|^2}{\sum_{F'=1}^2 \sum_{m'=-F'}^{F'} |\langle ^2P_{3/2}, F=2, m=2 | \mathbf{d} | ^2S_{1/2}, F', m' \rangle|^2}, \quad (4)$$

where  $\mathbf{d}$  is the operator of atomic dipole moment. The physical meaning of Eqs. (4) is transparent. For instance, the rate  $\gamma_{31}$  of transition from state  $|^2P_{3/2}, F=2, m=2\rangle$  into state  $|^2S_{1/2}, F=1, m=1\rangle$  with photon emission is equal to the product of  $\gamma$  by the ratio between the square of the dipole moment of this transition (which is proportional to the probability of just this transition) and the summed squares of the dipole moments of transitions from state  $|^2P_{3/2}, F=2, m=2\rangle$  onto every magnetic sublevel of states  $^2S_{1/2}$  with  $F=1$  and  $F=2$ . Simple calculations, which use the values of dipole moment matrix elements given in work [13], bring about  $\gamma_{31} = \gamma/2$  and  $\gamma_{32} = \gamma/6$ .

The field  $E$  that acts upon the atom takes the form

$$E = \frac{1}{2} \tilde{E}(t) e^{i\omega t} + \text{c.c.}, \quad (5)$$

where  $\tilde{E}(t)$  is the slowly varying complex amplitude of the field. Its expansion into a Fourier series looks like

$$\tilde{E}(t) = \sum_{n=-N_{\text{max}}}^{N_{\text{max}}} E_n \exp^{in\Omega_M t + i\phi_n}, \quad (6)$$

where  $\Omega_M = 2\pi/T$ . The Fourier amplitudes are simulated by the Gaussian-like distribution, and the phases by a function linear in  $n$ , which corresponds to the sequence of femtosecond pulses:

$$E_n = E_0 \exp\left(-\frac{n^2}{n_0^2}\right), \quad \phi_n = \beta n + \phi_0. \quad (7)$$

The variation of  $\beta$  or  $\phi_0$  is evidently equivalent to a time reckoning shift and does not influence the evolution of the state population in the atom interacting with the field. Therefore, in what follows, we put  $\beta = 0$  and  $\phi_0 = 0$ .

Let us introduce ‘‘irreducible’’ Rabi frequencies  $\Omega_n$  which are determined by the Fourier components of the field:

$$\Omega_n = -d_{\text{irr}} E_n / \hbar, \quad (8)$$

where  $d_{\text{irr}} = \langle ^2S_{1/2} | \mathbf{d} | ^2P_{3/2} \rangle$  is the irreducible matrix element of the dipole moment of transition  $^2S_{1/2} \leftrightarrow ^2P_{3/2}$ . If  $I_n$  is the intensity of the  $n$ -th Fourier component of the field, then [14]

$$\left| \frac{\Omega_n}{2\pi} [\text{MHz}] \right| = 70.24 \frac{d_{\text{irr}}}{ea_0} \sqrt{I_n [\text{W/cm}^2]}, \quad (9)$$

where  $e$  is the electron charge, and  $a_0$  the Bohr radius. For the transition  $^2S_{1/2} \leftrightarrow ^2P_{3/2}$ ,  $d_{\text{irr}} = 4.227 ea_0$  [13].

We need a stationary solution of Eqs. (1). For this purpose, the density matrix elements are expanded into Fourier series:

$$\rho_{11}(t) = \sum_{p=-\infty}^{\infty} \varrho_{11}^{(p)} e^{ip\Omega_M t}, \quad \rho_{12}(t) = \sum_{p=-\infty}^{\infty} \varrho_{12}^{(p)} e^{ip\Omega_M t},$$

$$\rho_{22}(t) = \sum_{p=-\infty}^{\infty} \varrho_{22}^{(p)} e^{ip\Omega_M t}, \quad \rho_{23}(t) = \sum_{p=-\infty}^{\infty} \varrho_{23}^{(p)} e^{i\omega t + ip\Omega_M t},$$

$$\rho_{33}(t) = \sum_{p=-\infty}^{\infty} \varrho_{33}^{(p)} e^{ip\Omega_M t}, \quad \rho_{13}(t) = \sum_{p=-\infty}^{\infty} \varrho_{13}^{(p)} e^{i\omega t + ip\Omega_M t}. \quad (10)$$

Substituting expansions (10) into Eqs. (1) and applying the approximation of circularly polarized wave, we obtain

$$\begin{aligned}
& \varrho_{11}^{(p)} (ip\Omega_M + \Gamma_{11}) - \Gamma_{11}\rho_{11}^{(0)} - \gamma_{31}\varrho_{33}^{(p)} + \\
& + \frac{i}{2} \sum_{q=-\infty}^{\infty} \Omega_{13}^{(q)} \left( \varrho_{31}^{(p-q)} e^{i\phi_q} - \varrho_{13}^{(p+q)} e^{-i\phi_q} \right) = 0, \\
& \varrho_{22}^{(p)} (ip\Omega_M + \Gamma_{22}) - \Gamma_{22}\rho_{22}^{(0)} - \gamma_{32}\varrho_{33}^{(p)} + \\
& + \frac{i}{2} \sum_{q=-\infty}^{\infty} \Omega_{23}^{(q)} \left( \varrho_{32}^{(p-q)} e^{i\phi_q} - \varrho_{23}^{(p+q)} e^{-i\phi_q} \right) = 0, \\
& \varrho_{33}^{(p)} (ip\Omega_M + \gamma_{31} + \gamma_{32} + \gamma_{3L}) + \\
& + \frac{i}{2} \sum_{q=-\infty}^{\infty} \Omega_{13}^{(q)} \left( \varrho_{31}^{(p-q)} e^{i\phi_q} - \varrho_{13}^{(p+q)} e^{-i\phi_q} \right) - \\
& - \frac{i}{2} \sum_{q=-\infty}^{\infty} \Omega_{23}^{(q)} \left( \varrho_{32}^{(p-q)} e^{i\phi_q} - \varrho_{23}^{(p+q)} e^{-i\phi_q} \right) = 0, \\
& \varrho_{12}^{(p)} \left[ ip\Omega_M - i\omega_{12} + \frac{1}{2} (\Gamma_{11} + \Gamma_{22}) \right] + \\
& + \frac{i}{2} \sum_{q=-\infty}^{\infty} \left( \Omega_{13}^{(q)} \varrho_{32}^{(p-q)} e^{i\phi_q} - \Omega_{23}^{(q)} \varrho_{13}^{(p+q)} e^{-i\phi_q} \right) = 0, \\
& \varrho_{13}^{(p)} \left[ ip\Omega_M + i\delta + \frac{1}{2} (\Gamma_{11} + \gamma_{31} + \gamma_{32} + \gamma_{3L}) \right] + \\
& + \frac{i}{2} \sum_{q=-\infty}^{\infty} e^{i\phi_q} \left[ \Omega_{13}^{(q)} \left( \varrho_{33}^{(p-q)} - \varrho_{11}^{(p-q)} \right) - \Omega_{23}^{(q)} \varrho_{12}^{(p-q)} \right] = 0, \\
& \varrho_{23}^{(p)} \left[ ip\Omega_M + i\delta + \omega_{12} + \frac{1}{2} (\Gamma_{22} + \gamma_{31} + \gamma_{32} + \gamma_{3L}) \right] + \\
& + \frac{i}{2} \sum_{q=-\infty}^{\infty} e^{i\phi_q} \left[ \Omega_{23}^{(q)} \left( \varrho_{33}^{(p-q)} - \varrho_{22}^{(p-q)} \right) - \Omega_{13}^{(q)} \varrho_{21}^{(p-q)} \right] = 0, \\
& \varrho_{21}^{(p)} = \left( \varrho_{12}^{(-p)} \right)^*, \varrho_{31}^{(p)} = \left( \varrho_{13}^{(-p)} \right)^*, \varrho_{32}^{(p)} = \left( \varrho_{23}^{(-p)} \right)^*, \quad (11)
\end{aligned}$$

where

$$\delta = \omega - \frac{W_3 - W_1}{\hbar}, \quad \omega_{12} = \frac{W_2 - W_1}{\hbar}, \quad (12)$$

and

$$\begin{aligned}
\Omega_{13}^{(n)} &= -\frac{d_{13}E_n}{\hbar} = \frac{d_{13}}{d_{\text{irr}}} \Omega_n = \frac{1}{2} \Omega_n, \\
\Omega_{23}^{(n)} &= -\frac{d_{23}E_n}{\hbar} = \frac{d_{23}}{d_{\text{irr}}} \Omega_n = \sqrt{\frac{1}{12}} \Omega_n. \quad (13)
\end{aligned}$$

The obtained equations (11) cannot be solved analytically. We use them below for a numerical simulation of dark resonances in the fluorescence intensity produced by Rb vapor in a cell in a field of femtosecond laser pulses. Instead of changing the pulse repetition period  $T$ , the appropriate choice of which leads to a dip in the dependence of the fluorescence intensity on  $T$ , we consider the dependence of the fluorescence intensity on the magnetic field induction  $B$ , the variation of which detunes the difference between the energies of states  $|1\rangle$  and  $|2\rangle$  from the condition of resonance with one of the differences between the frequencies of Fourier components of the laser radiation field.

### 3. Numerical Simulation of a Dark Resonance

The population  $n_3$  of state  $|3\rangle = |^2P_{3/2}, F=2, m=2\rangle$  at the interaction between a Rb atom and the  $\sigma^+$ -polarized radiation of a femtosecond laser is found by solving Eqs. (11). Only two Fourier components of the laser radiation, which are the closest to the frequencies of transitions  $|1\rangle \leftrightarrow |3\rangle$  and  $|2\rangle \leftrightarrow |3\rangle$  are taken into account. The femtosecond laser radiation emission wavelength  $\lambda = 780.24$  nm, and the pulse repetition frequency is about 75.65 MHz. For a numerical simulation, we have to know the Rabi frequency  $\Omega_0$  and the relaxation constants  $\Gamma_{11}$  and  $\Gamma_{22}$ . For estimations, let us take  $\Gamma_{11} = \Gamma_{22} = 1/\tau_{\text{tr}}$ , where  $\tau_{\text{tr}}$  is the time needed for an atom to cross the laser beam. The one-mode power of laser radiation emission was 2.3  $\mu\text{W}$ . With the help of a lens, it was possible to vary the laser beam diameter at the site of its interaction with rubidium atoms. Equation (9) makes it possible to calculate  $\Omega_0$ . For instance, in the case of the laser beam diameter  $2R = 8$  mm, we have  $\Omega_0/2\pi = 0.64$  MHz. For the numerical simulation, we selected the pulse repetition frequency  $\nu = 75.65$  MHz. On the one hand, the beam focusing increases  $\Omega_0$ ; on the other hand, it reduces  $\tau_{\text{tr}}$ .

If the magnetic field is absent, the energy difference  $W_2 - W_1$  is 6834.682610904 MHz in terms of frequency

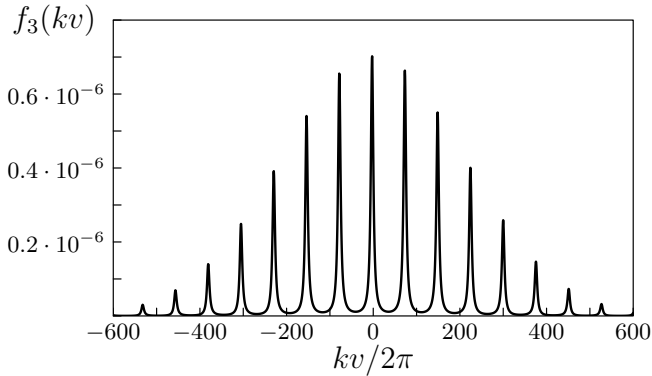


Fig. 2. Distribution function of rubidium atoms over their velocities in state  $|^2P_{3/2}, F=2, m=2\rangle$ . The diameter of a laser beam  $2R = 8$  mm,  $B = -18.766$  Gs

units [13]. The field-induced energy variation of the state characterized by the quantum numbers  $F$  and  $m$  is determined by the expression

$$\Delta W_{|F,m\rangle} = \mu_B g_F m B, \quad (14)$$

where  $B$  is the projection of the vector of magnetic induction onto the direction of light propagation. For state  $|^2S_{1/2}, F=1\rangle$ , we have  $\mu_B g_F = -0.7$  MHz/Gs; for state  $|^2S_{1/2}, F=2\rangle$ ,  $\mu_B g_F = 0.7$  MHz/Gs; and for state  $|^2P_{3/2}, F=1, 2, 3\rangle$ ,  $\mu_B g_F = 0.93$  MHz/Gs [13]. Whence, it follows that, when the  $\sigma^+$ -polarized radiation interacts with a Rb atom, a dark resonance for the state  $|^2P_{3/2}, F=2, m=2\rangle$  population is to be observed at  $B = -18.766$  Gs (the energy difference between sublevels with  $m=1$  is  $90h\nu$ ). The main contribution to the dark resonance formation is given by those atoms, the speeds of which, owing to the Doppler effect, provide the resonance interaction between the Fourier components of the field and the atom. Let us check up our assumption that the influence of level  $|^2P_{3/2}, F=3, m=2\rangle$  on the resonance formation can be neglected. Taking into account that the energy difference between levels  $|^2P_{3/2}, F=2, m=2\rangle$  and  $|^2P_{3/2}, F=3, m=2\rangle$  is 266.650 MHz in frequency units, we obtain that the detuning of the Fourier component of the spectrum closest to the frequency of transition  $|^2S_{1/2}, F=1, m=1\rangle \leftrightarrow |^2P_{3/2}, F=3, m=2\rangle$  is about 35 MHz, which considerably exceeds the inverse lifetime of an atom in the excited state (of about 6 MHz).

In our calculations, we took the distribution of atoms over their velocities into account. At room temperature, the root-mean-square velocity of the atom  $v_0 = 280$  m/s, so that  $kv_0 \approx 300$  MHz. The time of atom transit through the laser beam  $\tau_{tr} = 2R/v_0$ . The relaxation rates  $\Gamma_{11} = \Gamma_{22} = 1/\tau_{tr} = 50$  kHz at  $2R = 8$  mm. The

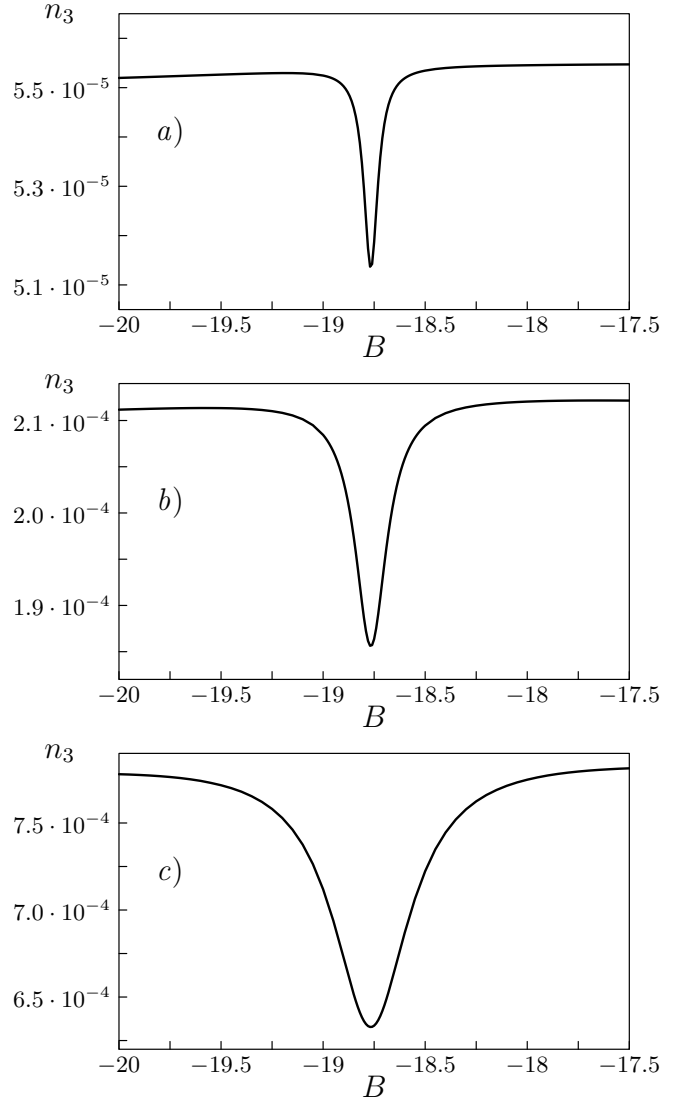


Fig. 3. Results of numerical calculations of the dependences of the population of state  $|^2P_{3/2}, F=2, m=2\rangle$  on the magnetic field induction (in Gs) for various diameters of a laser beam  $2R = 8$  (a), 4 (b), and 2 mm (c), which correspond to  $\Omega_0/2\pi = 0.65, 1.3,$  and  $2.6$  MHz, and  $\Gamma_{11}/2\pi = \Gamma_{22}/2\pi = 50, 100,$  and  $200$  kHz, respectively

halfwidth of line  $D2$ , which arises due to the distribution of atoms over their velocities (the Doppler broadening), considerably exceeds the pulse repetition frequency. As a result, several groups of atoms with different velocities give a contribution to the formation of a dark resonance (see Fig. 2), and the population of the excited state becomes much higher than it could be at the interaction between the atom and a bichromatic field.

In Fig. 3, the dependences of the population of state  $|^2P_{3/2}, F=2, m=2\rangle$  on the magnetic field induction are

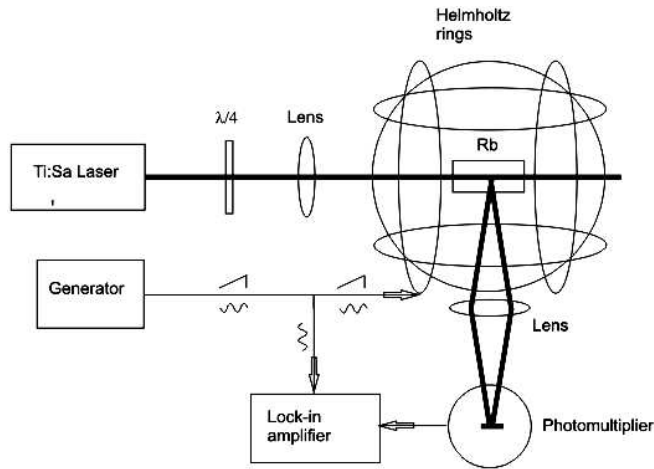


Fig. 4. Scheme of the experimental installation

depicted for various diameters of the laser beam, namely,  $2R = 8, 4,$  and  $2$  mm, which correspond to  $\Omega_0/2\pi = 0.65, 1.3,$  and  $2.6$  MHz, and  $\Gamma_{11}/2\pi = \Gamma_{22}/2\pi = 50, 100,$  and  $200$  kHz, respectively. The contrast (the ratio between the dip depth and the value beyond the dip) of the dark resonance in the dependence of the population of state  $|3\rangle$  on the magnetic field is equal to  $0.07, 0.12,$  and  $0.18$  for cases  $a, b,$  and  $c,$  respectively.

Note that a dark resonance can also be observed for the transitions from states  $|^2S_{1/2}, F = 1, m = -1\rangle$  and  $|^2S_{1/2}, F = 2, m = -1\rangle$  into states  $|^2P_{3/2}, F = 2, m = 0\rangle$  and  $|^2P_{3/2}, F = 2, m = 0\rangle,$  when two  $\Lambda$ -schemes of atom-field interaction are realized simultaneously. Since, in this case, the magnetic quantum number of the ground state is the same by the absolute value as that in the case just analyzed by us, the dark resonance will be observed at the same value  $B = 18.766$  Gs, but at another direction of the magnetic field induction. It is essential that, when one of the  $\Lambda$ -schemes is close to a single-photon resonance, the detuning of the other  $\Lambda$ -scheme from the single-photon resonance amounts to  $5.7$  MHz, which is close to the line width of Rb-atom fluorescence. The conditions, which are needed for the registration of this dark resonance, are evidently less favorable than those in the case where atoms occupying the magnetic sublevels of the ground state with  $m = 1$  are excited. The analysis of the four-level scheme, which is similar to that in the three-level case, gives a resonance contrast of about  $0.11$  for the dependence of the total population in states  $|^2P_{3/2}, F = 1, m = 0\rangle$  and  $|^2P_{3/2}, F = 2, m = 0\rangle$  on the magnetic field in the case where the diameter of a laser beam is  $2$  mm.

The other states also contribute to atomic fluorescence, which reduces the dark resonance contrast. For example, for  $2R = 2$  mm, the dark resonance in the dependence of the total population on magnetic sublevels of states  $|^2P_{3/2}, F = 1\rangle$  and  $|^2P_{3/2}, F = 2\rangle$  has a contrast of  $0.05$  at the interaction between the atom and the  $\sigma^+$ -polarized light.

For the observation of a dark resonance, a femtosecond laser with the wavelength  $\lambda = 780.24$  nm was used. By filtering the laser radiation, a spectral interval of about  $\Delta\lambda = 0.2$  nm was selected. The radiation power in this spectral interval was  $3$  mW. The pulse repetition frequency  $\nu$  was different in every experiment, by varying around  $75.65$  MHz. This means that the radiation that acted upon the atom consisted of  $N = c\Delta\lambda/\lambda^2\Delta\nu = 1300$  modes, and the power of a mode was  $P = 3000 \mu\text{W}/1300 = 2.3 \mu\text{W}.$

The scheme of the experimental installation is shown in Fig. 4. A beam about  $6$  mm in diameter generated by a femtosecond laser passed through a quarter-wave plate to be focused by a lens with a focal length of  $40$  cm in a cell with rubidium vapor (the natural mixture of isotopes  $^{87}\text{Rb}:^{85}\text{Rb}=27.835\%:72.165\%$  [16]) at a temperature of  $25^\circ\text{C}.$  The laser beam diameter at the fluorescence registration site was about  $2$  mm, so that the intensity of one mode was  $I = P/(\pi R^2) = 73 \times 10^{-6} \text{ W/cm}^2.$  Using formula (9), we obtain  $\Omega_n/2\pi = \Omega_0/2\pi = 2.6$  MHz (in a narrow spectral interval of laser radiation, which acted upon the atom, the intensities of Fourier components practically did not differ from one another). Fluorescence of rubidium was registered by means of a photoelectronic multiplier. The cell was located at the center of a system of Helmholtz rings, two pairs of which were used to compensate the Earth's magnetic field, and the third pair created the working magnetic field along the direction of beam propagation. The block of the current control by means of Helmholtz rings allowed us to scan the magnetic field in accordance with a triangular signal given by an external generator and also to modulate the field with a frequency of  $900$  Hz. The deviation amplitude was  $0.2$  Gs. The signal from a photoelectronic multiplier was synchronously detected at the same frequency of  $900$  Hz and recorded into the computer memory with the help of an ADC. To register the current in the coils, and, respectively, the magnetic field magnitudes in rubidium vapor, the voltage drop across a resistor connected in series with the coils was measured.

According to our calculations (Fig. 3,c), the dark resonance width should be about  $1$  Gs. Its position is determined by the pulse repetition frequency and changes

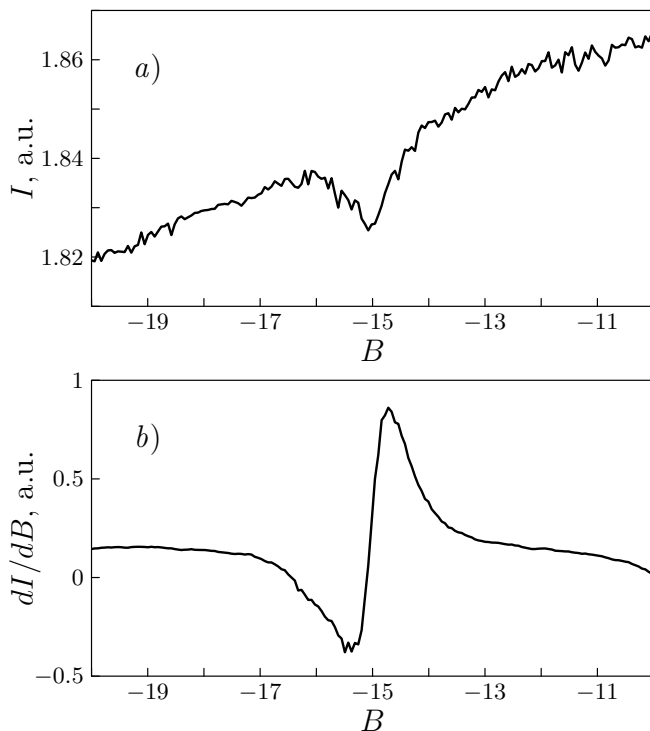


Fig. 5. Dependences of the fluorescence intensity  $I$  (a) and the derivative  $dI/dB$  averaged over the interval of the order of  $B$ -deviation amplitude (b) on the magnetic field induction  $B$  (in Gs)

from  $-21.9$  to  $-15.5$  Gs, if the frequency varies from  $75.6$  to  $75.7$  MHz. The dependences of the fluorescence intensity  $I$  (in arbitrary units) and the derivative  $dI/dB$  averaged over an interval of the order of the deviation amplitude (the signal from a synchronous detector) on the magnetic field induction, which are exhibited in Fig. 5, correspond to the laser pulse repetition frequency of  $75.71$  MHz. The dark resonance width (of about  $1.5$  Gs), as is seen from Fig. 5, *a*, agrees well with the results of theoretical calculations. The resonance contrast (the ratio between the dip depth and the value beyond the dip) is slightly larger than  $1.5\%$ , which is close, by the order of magnitude, to the theoretical value of  $5\%$  given at the end of Section 3.

#### 4. Conclusions

Dark resonances, which are observed at the interaction of rubidium vapor with a femtosecond laser radiation, have been studied both theoretically and experimentally. Dark resonances have been observed for the first time at frequencies that correspond to line  $D2$  in the fluorescence

spectrum of  $^{87}\text{Rb}$  vapor. The experimental data agree well with the results of numerical simulations of the interaction between the Rb atom and the laser radiation field.

The work was carried out in the framework of the INTAS project 06-100024-9075 and DFFD-RFFD project F28.2/035.

1. G. Alzetta, A. Gozzini, L. Moi, and G. Orriols, *Nuovo Cimento B* **36**, 5 (1976).
2. E. Arimondo and G. Orriols, *Lett. Nuovo Cimento* **17**, 333 (1976).
3. H.R. Gray, R.W. Whitley, and C.R. Stroud, jr., *Opt. Lett.* **3**, 218 (1978).
4. B.W. Shore, *Acta Phys. Slov.* **58**, 243 (2008); see <http://www.physics.sk/aps/pub.php?y=2008&pub=aps-08-03>
5. M. Erhard and H. Helm, *Phys. Rev. A* **63**, 043814 (2001).
6. S. Knappe, R. Wynands, J. Kitching, H.G. Robinson, and L. Hollberg, *J. Opt. Soc. Am. B* **18**, 1545 (2001).
7. A. Nagel, L. Graf, F. Naumov, E. Mariotti, V. Biancalana, D. Meschede, and R. Wynands, *Europhys. Lett.* **44**, 31 (1998).
8. P.D.D. Schwindt, S. Knappe, V. Shah, L. Hollberg, J. Kitching, L.-A. Liew, and J. Moreland, *Appl. Phys. Lett.* **85**, 6409 (2004).
9. L. Arissian and J.-C. Diels, *Optics Communications* **264**, 169 (2006).
10. Yu.V. Vladimirova, B.A. Grishanin, V.N. Zadkov, V. Byankalana, D. Bevilakva, Y. Dancheva, and L. Moi, *Zh. Eksp. Teor. Fiz.* **130**, 609 (2006).
11. S.T. Cundiff and F.J. Ye, *Rev. Mod. Phys.* **75**, 325 (2003).
12. S.V. Borisenok and Yu.V. Rozhdestvenskii, *Zh. Eksp. Teor. Fiz.* **123**, 5 (2003).
13. D.A. Steck, <http://steck.us/alkalidata>.
14. B.W. Shore, *The Theory of Coherent Atomic Excitation* (Wiley, New York, 1990).
15. L.P. Yatsenko, B.W. Shore, and K. Bergmann, *Opt. Commun.* **236**, 183 (2004).
16. *Physical Encyclopedia*, edited by A.M. Prokhorov (Bol'sh. Ross. Entsycl., Moscow, 1994), Vol. 4 (in Russian).

Received 22.12.08.

Translated from Ukrainian by O.I. Voitenko

ДОСЛІДЖЕННЯ ТЕМНИХ РЕЗОНАНСІВ В АТОМАХ  
РУБІДІЮ У ПОЛІ ПОСЛІДОВНОСТЕЙ СВІТЛОВИХ  
ІМПУЛЬСІВ

*М. Аузіньш, Р.А. Маліцький, І.В. Мацнев, А.М. Негрійко,  
В.І. Романенко, В.М. Ходаковський, Л.П. Яценко*

Резюме

Теоретично і експериментально досліджено темні резонанси в парі  $^{87}\text{Rb}$  у полі послідовності фемтосекундних лазерних

імпульсів. Аналізуються три- і чотирирівнева схеми взаємодії атома з полем, сформовані пов'язаними полем магнітними підрівнями станів  $^2S_{1/2}$ ,  $^3P_{3/2}$  атома  $^{87}\text{Rb}$ . Положення і форма експериментально зареєстрованого темного резонансу відповідає проведеним розрахункам. Показано, що взаємодія пари рубідію з поліхроматичним полем дозволяє значно збільшити величину сигналу порівняно з випадком біхроматичного поля.